

Effect of variation Mn/W molar ratios on phase composition, morphology and optical properties of MnWO_4

Sen Zhou, Jianfeng Huang*, Ting Zhang, Haibo Ouyang, Ating Li, Zhenwei Zhang

School of Materials Science and Engineering, Shaanxi University of Science and Technology, Xi'an 710021, PR China

Received 31 October 2012; received in revised form 15 November 2012; accepted 5 December 2012

Available online 12 December 2012

Abstract

Manganese tungstate (MnWO_4) particles were successfully synthesized by a microwave hydrothermal method using $\text{MnCl}_2 \cdot 4\text{H}_2\text{O}$ and $\text{Na}_2\text{WO}_4 \cdot 2\text{H}_2\text{O}$ as the starting materials. The products were characterized by X-ray diffraction, field-emission scanning electron microscopy, transmission electron microscopy and UV–vis absorption spectra. Results show that pure MnWO_4 particles can be fabricated in the Mn/W molar ratio range from 1:2 to 2:1. The crystallinity of MnWO_4 increases first and then decreases with increasing Mn/W molar ratio. MnWO_4 morphology transforms from nanorods to aggregated spheres. UV–vis absorption spectra of these two morphologies exhibit a distinct redshift compared with bulk MnWO_4 . The band gaps of the nanorods and aggregated spheres-like MnWO_4 particles are 2.75 eV and 2.65 eV, respectively.

© 2012 Elsevier Ltd and Techna Group S.r.l. All rights reserved.

Keywords: Microwave hydrothermal method; Mn/W molar ratios; MnWO_4 ; Optical property

1. Introduction

Considerable interest has been focused recently on the fabrication of nano/microstructure materials, mainly because of their unique electronic, optical and magnetic properties, and potential applications [1–3]. As one of the most important semiconductors, Manganese tungstate (MnWO_4) is a promising material with potential applications in many fields, such as photoluminescence [4], humidity sensors [5], magnetic materials [6], photocatalysts [7] etc. It is well known that the morphology and size have extensive influence on the physical and chemical properties of MnWO_4 [8]. Hence, synthesis of nano/microstructure MnWO_4 with different morphologies has become a focus in the reported researches. Up to now, a lot of methods have been developed to prepare MnWO_4 , including hydrothermal method [7], solvothermal method [9], aqueous reaction method [10], sol–gel method [11], low-temperature molten salt method [12], surfactant-assisted complexation-precipitation method [13], and cyclic

microwave-assisted spray synthesis method [14]. However, the above methods have such limitations as high reaction temperature, long reaction time, poor reaction efficiency, high heat treatment temperature, the need of adding surfactant and even dangerous organic solvents as well as pretreating substrate. One approach to overcome these drawbacks is the microwave-hydrothermal method. This method has some advantages such as heating throughout the media, rapid heating, fast reaction, high yield, excellent reproducibility, narrow particle distribution, high purity and high efficient energy transformation [15,16]. Recently, MnWO_4 with rod-like and flake-like structure produced by microwave hydrothermal method was synthesized by Almeida et al. [2,4]. Even though they have prepared MnWO_4 by using microwave hydrothermal method, they added different surfactants [cetyltrimethylammonium bromide (CTAB), sodium dodecyl sulfate (SDS) and sodium bis (2-ethylhexyl) sulfosuccinate (AOT)] and have not investigated the effect of variation Mn/W molar ratio on the morphology and property of MnWO_4 .

In the present work, MnWO_4 particles have been synthesized just by adjusting Mn/W molar ratios of microwave precursor with a facile, quick, environmental microwave

*Corresponding author. Tel./fax: +86 029 8616 8802.

E-mail addresses: zhousen303@163.com (S. Zhou), hjfnpu@163.com (J. Huang).

hydrothermal method without any metal catalyst, template or surfactant. In addition, the optical absorption properties of nanorods and spheres-like MnWO_4 were investigated.

2. Experimental

All chemicals were analytical grade and used as received without further purification. In a typical synthesis process, $\text{Na}_2\text{WO}_4 \cdot 2\text{H}_2\text{O}$ (5 mmol) and $\text{MnCl}_2 \cdot 4\text{H}_2\text{O}$ (5 mmol) were dissolved in deionized water (25 mL), respectively. The Na_2WO_4 solution was added into the MnCl_2 solution slowly under stirring, which resulted in a white precipitate. The solution pH was adjusted to 9 with NaOH (1 mol/L) solution. The mixture was sealed in a 100 mL Teflon-lined autoclave. This autoclave was then put into a MDS-8 microwave hydrothermal system (Shanghai Sineo Microwave Chemistry Technology Co. Ltd., China). The operating power was set to 400 W. The system was set to the temperature-controlled mode to maintain at 160 °C for 40 min. Afterward, the as-prepared brown precipitates were isolated by centrifugation and washed with deionized water and absolute ethanol for several times. Finally, the brown precipitates were dried at 60 °C in a drying cabinet for 6 h. To investigate the effects of different Mn/W molar ratios on the phase composition and morphology of the products, the content of Mn^{2+} changed from 2.5 mmol to 15 mmol (Mn/W molar ratio from 1:2 to 3:1, respectively) without changing the content of WO_4^{2-} .

The phase composition of the samples was characterized via X-ray diffraction (XRD) on a D/MAX-2200PC X-ray diffractometer with $\text{CuK}\alpha$ radiation ($\lambda = 0.15406$ nm) at a scanning rate of 8°min^{-1} (Rigaku, Japan). Field-emission scanning electron microscope (FESEM, S-4800, Japan) and transmission electron microscope (TEM, JEM-3010, Japan) were used to analyze the product morphology and microstructures. Further structural characterization was performed on high-resolution transmission electron microscope (HRTEM, JEM-3010, Japan). UV–vis absorption spectra were recorded on a Lambda 950 spectrophotometer.

3. Results and discussion

3.1. Analysis of phase composition

The influence of the Mn/W molar ratios on the phase composition of products has been investigated by XRD. Fig. 1 shows the XRD patterns of as-prepared samples at different Mn/W molar ratio from 1:2 to 3:1. According to the XRD patterns, pure crystalline MnWO_4 was obtained at Mn/W molar ratios equal to 1:2, 1:1 and 2:1. All reflection peaks of the different products can be easily indexed as a pure, monoclinic wolframite tungstate structure with cell parameters MnWO_4 : $a = 0.48277$ nm, $b = 0.57610$ nm, $c = 0.49970$ nm, $\alpha = \gamma = 90^\circ$, and $\beta = 91.14^\circ$, which are consistent with literature values (JCPDS Card Number: 80-0133). The intensity of main reflection peaks of products increased first and then decreased with the increase of Mn/W molar ratio, which indicates the crystallinity of

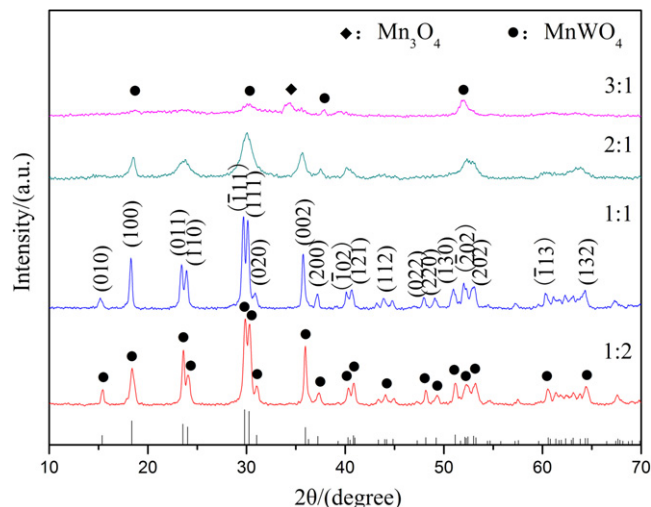


Fig. 1. XRD patterns of the MnWO_4 prepared at different Mn/W molar ratio values.

MnWO_4 increased first and then decreased. Moreover, the main reflection peaks of all pure MnWO_4 has a trend to shift to low-angles slightly compared with standard cards (on abscissa axis), which illustrates the cell parameters increased. When Mn/W molar ratio increased from 1:2 to 1:1, the intensity of main reflection peaks of MnWO_4 not only increased but also became narrower and sharper. Therefore the crystallinity and grain size of the product increased. At Mn/W molar ratio equal to 2:1, the intensity of main reflection peaks of MnWO_4 got broadened and weakened, which illustrates its crystallinity and grain size decreased. At Mn/W molar ratio equal to 3:1, a little of Mn_3O_4 phase generated besides MnWO_4 phase in the product. It is probable that Mn^{2+} and OH^- combine to form $\text{Mn}(\text{OH})_2$. However, $\text{Mn}(\text{OH})_2$ is not stable, easy to be oxidized to Mn_3O_4 by O_2 [17]. Therefore, it is conducive to the preparation of pure phase MnWO_4 at Mn/W molar ratio from 1:2 to 2:1.

3.2. Morphologies of MnWO_4 crystallites

TEM and HRTEM images of MnWO_4 crystallites prepared at Mn/W molar ratio equal to 1:2 and 1:1 are shown in Fig. 2. It can be observed that the morphology of MnWO_4 is a nanorod from Fig. 2(a) and (b). At Mn/W molar ratio equal to 1:2, the length and width of nanorods are 30–130 nm and 15–40 nm. At Mn/W molar ratio equal to 1:1, the length and width of nanorods are 40–200 nm and width 15–40 nm. With the increase of Mn/W molar ratio, grain size and crystallinity of products increased, which are in good agreement with the results of XRD analysis. To understand the preferential orientation growth, MnWO_4 samples have been further studied using high-resolution TEM (HRTEM), and the results (one of nanorods in Fig. 2(b)) are shown in Fig. 2(c). HRTEM image indicates that MnWO_4 nanorods existed as a single-crystal structure. It is in accordance with the SAED (inset of Fig. 2 (c)) results. The lattice spacings of orthogonal lattice 0.490 and

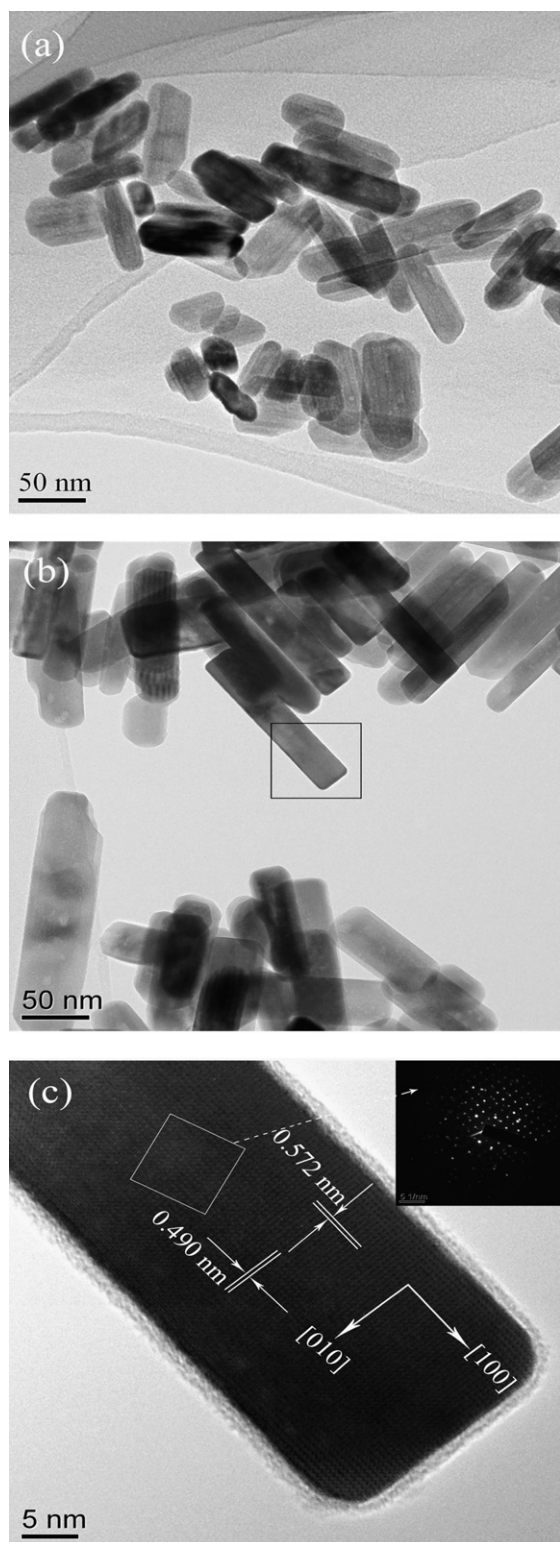


Fig. 2. (a), (b) TEM images of MnWO_4 prepared at Mn/W molar ratio equal to 1:2, 1:1, respectively, and (c) HRTEM image of a nanorod in (b) (inset shows the SAED image).

0.572 nm corresponded to the (100) and (010) planes of the MnWO_4 monoclinic cell, respectively. In conclusion, nanorods grew along the [100] direction.

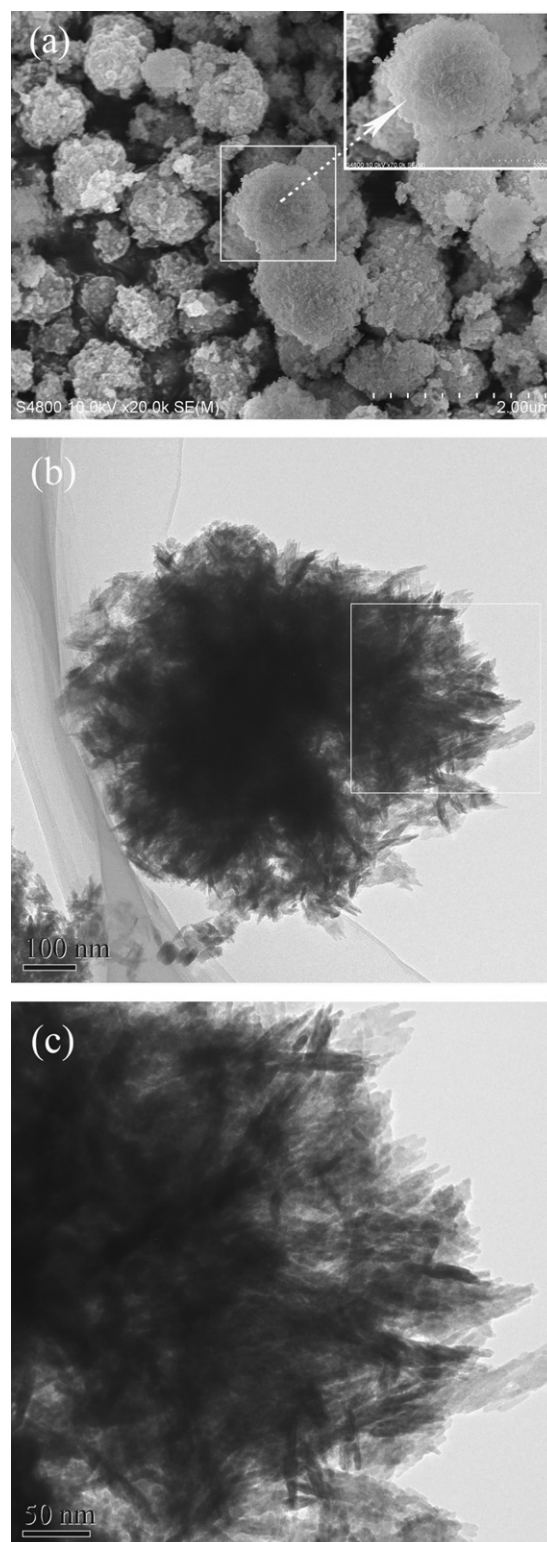


Fig. 3. FESEM and TEM images of MnWO_4 crystallites prepared at Mn/W molar ratio equal to 2:1.

FESEM and TEM images of MnWO_4 crystallites prepared at Mn/W molar ratio equal to 2:1 are shown in Fig. 3. It can be observed that the product is composed of sphere-like microcrystallites from Fig. 3(a). From the view

of partial enlarged image of individual particle (inset of Fig. 3(a)), the MnWO_4 microcrystallites are not single grains, but sphere-like aggregates. Fig. 3(b) and (c) are TEM image and partial enlarged image of a sphere-like particle, respectively. It shows that sphere-like MnWO_4 particles were aggregated by abundant smaller nanorods with poor crystallinity, which is in accordance with XRD results. It is well known that the mean crystal diameter or mean particle diameter of samples decreases while specific surface area increases. Therefore, the specific surface free energy is higher. In order to reduce its specific surface free energy, the smaller nanorods will aggregate to form sphere-like particles by surface adsorption.

3.3. Optical properties of the MnWO_4 with different structures

The typical optical absorption spectra of the as-prepared samples at Mn/W molar ratio equal to 1:1 and 2:1 respectively are presented in Fig. 4(a). Both spheres and nanorods not only have a strong and broad absorption in the ultraviolet spectrum but also have a certain absorption in

the visible region from 400 to 800 nm to show great potential applications in the fields of photocatalytic and photoluminescence etc. As MnWO_4 is a direct band gap semiconductor, therefore its absorption the relationship between the adsorption coefficient (α) near the absorption edge and the optical band gap (E_g) obeys the following formula $(\alpha h\nu)^2 = A(h\nu - E_g)$ [18], where $h\nu$ is the incident photon energy, and A is a constant. Thus, as is illustrated in Fig. 4(b), the band gap for spheres MnWO_4 is 2.65 eV, while the band gap for nanorods MnWO_4 is 2.75 eV. Compared with the band gap for bulk MnWO_4 [19] (2.8 eV), they exhibited a distinct redshift, which may result from the internal stress generated in the process, crystallinity of products and orientation growth of crystal etc. In conclusion, the band gaps of MnWO_4 nanorod and sphere assembled structure is strongly related to the morphology of products. The Mn/W molar ratios of microwave hydrothermal precursor have great effect on the morphology of MnWO_4 .

4. Conclusions

In summary, nanorods and aggregated spheres-like MnWO_4 particles have been successfully synthesized by a facile, quick, environmental microwave hydrothermal method without adding any metal catalyst, template or surfactant. The results show that the Mn/W molar ratio is found to greatly affect the product morphology and its phase. At Mn/W molar ratio from 1:2 to 1:1, MnWO_4 nanorods with a [100]-preferred orientation were obtained, and its crystallinity increased. At Mn/W molar ratio from 1:1 to 2:1, the morphology of products transformed from nanorods to spheres-like aggregated by abundant smaller nanorods. The UV–vis absorption spectra of these two morphologies exhibit a distinct redshift compared with bulk MnWO_4 . The optical band gap of 2.65 eV and 2.75 eV to aggregated spheres and nanorods MnWO_4 particles, respectively. This result indicates the optical performance of MnWO_4 particles is strongly related to the morphology of products. The Mn/W molar ratios of microwave hydrothermal precursor have great effect on the morphology of MnWO_4 .

Acknowledgments

This work was supported by the National Natural Science Foundation of China (50942047), Natural Science Foundation of Shaanxi Province of China (2010JM6001 and 2010JM6017), International Science and Technology Cooperation Project of Shaanxi Province (2011KW-11) and the Graduate Innovation Foundation of Shaanxi University of Science and Technology.

References

- [1] S. Saranya, S.T. Senthikumar, K.V. Sankar, R.K. Selvan, Synthesis of MnWO_4 nanorods and its electrical and electrochemical properties, *Journal of Electroceramics* 28 (2012) 220–225.

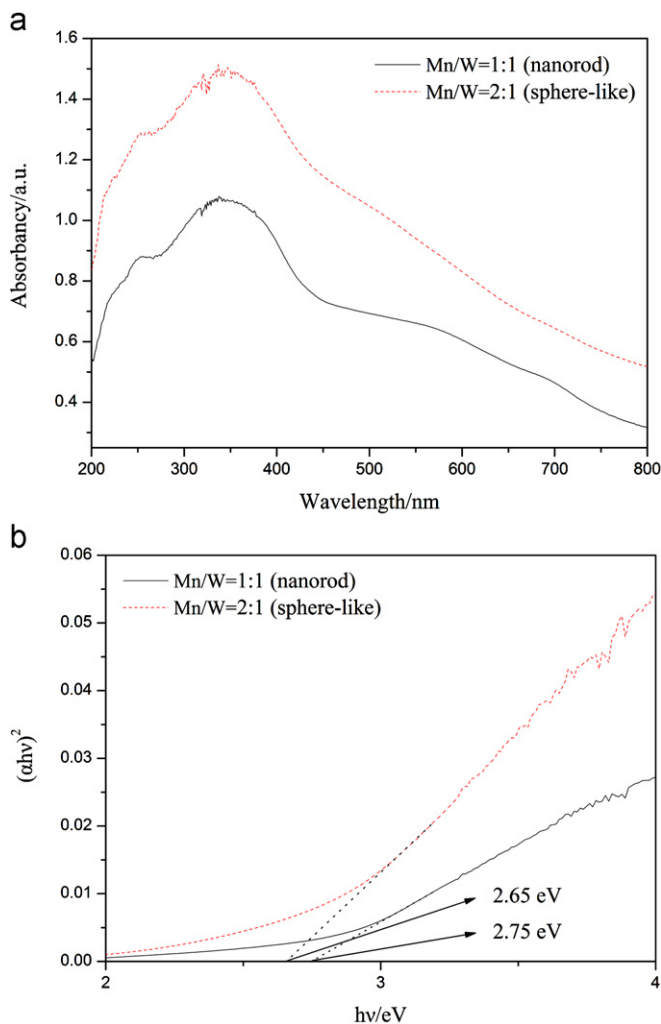


Fig. 4. (a) UV–vis absorption spectra of MnWO_4 with different morphologies and (b) the relationship between $(\alpha h\nu)^2$ and $h\nu$.

- [2] M.A.P. Almeida, L.S. Cavalcante, M. Siu Li, J.A. Varela, E. Longo, Structural refinement and photoluminescence properties of MnWO_4 nanorods obtained by microwave-hydrothermal synthesis, *Journal of Inorganic and Organometallic Polymers and Materials* 22 (2012) 264–271.
- [3] V. Felea, P. Lemmens, S. Yasin, S. Zherlitsyn, K.Y. Choi, C.T. Lin, Ch. Payen, Magnetic phase diagram of multiferroic MnWO_4 probed by ultrasound, *Journal of Physics: Condensed Matter* 23 (2011) 216001.
- [4] M.A.P. Almeida, L.S. Cavalcante, J.A. Varela, M. Siu Li, E. Longo, Effect of different surfactants on the shape, growth and photoluminescence behavior of MnWO_4 crystals synthesized by the microwave-hydrothermal method, *Advanced Powder Technology* 23 (2012) 124–128.
- [5] W. Qu, W. Wlodarski, J.U. Meyer, Comparative study on micro-morphology and humidity sensitive properties of thin-film and thick-film humidity sensors based on semiconducting MnWO_4 , *Sensors and Actuators B* 64 (2000) 76–82.
- [6] F. Ye, R.S. Fishman, J.A. Fernandez-Baca, A.A. Podlesnyak, G. Ehlers, H.A. Mook, Y.Q. Wang, B. Lorenz, C.W. Chu, Long-range magnetic interactions in the multiferroic antiferromagnet MnWO_4 , *Physical Review B* 83 (2011) 140401.
- [7] W.Q. Wu, W.H. Qin, Y.M. He, Y. Wu, T.H. Wu, The effect of pH value on the synthesis and photocatalytic performance of MnWO_4 nanostructure by hydrothermal method, *Journal of Experimental Nanoscience* 7 (2012) 390–398.
- [8] U. Dellwo, P. Keller, J.U. Meyer, Fabrication and analysis of a thick-film humidity sensor based on MnWO_4 , *Sensors and Actuators A* 61 (1997) 298–302.
- [9] S.J. Chen, X.T. Chen, Z.L. Xue, J.H. Zhou, J. Li, J.M. Hong, X.Z. You, Morphology control of MnWO_4 nanocrystals by a solvothermal route, *Journal of Materials Chemistry* 13 (2003) 1132–1135.
- [10] H.Y. He, J.F. Huang, L.Y. Cao, J.P. Wu, Photodegradation of methyl orange aqueous on MnWO_4 powder under different light resources and initial pH, *Desalination* 252 (2010) 66–70.
- [11] W. Qu, W. Wlodarski, J.U. Meyer, Comparative study on micro-morphology and humidity sensitive properties of thin-film and thick-film humidity sensors based on semiconducting MnWO_4 , *Sensors and Actuators B* 64 (2000) 76–82.
- [12] Z.W. Song, X.Y. Li, J.S. Shi, Synthesis of MnWO_4 nano-particles by low-temperature molten salt method, *Advanced Materials Research* 284–286 (2011) 722–725.
- [13] S.J. Lei, K.B. Tang, Z. Fang, Y.H. Huang, H.G. Zheng, Synthesis of MnWO_4 nanofibers by a surfactant-assisted complexation-precipitation approach and control of morphology, *Nanotechnology* 16 (2005) 2407–2411.
- [14] S. Thongtem, S. Wannapop, A. Phuruangrat, T. Thongtem, Cyclic microwave-assisted spray synthesis of nanostructured MnWO_4 , *Materials Letters* 63 (2009) 833–836.
- [15] S. Komarneni, R. Roy, Q.H. Li, Microwave-hydrothermal synthesis of ceramic powers, *Materials Research Bulletin* 27 (1992) 1393–1405.
- [16] X.C. Xu, Y. Bao, C.S. Song, W.S. Yang, J. Liu, L.W. Lin, Microwave-assisted hydrothermal synthesis of hydroxyl-sodalite zeolite membrane, *Microporous and Mesoporous Materials* 75 (2004) 173–181.
- [17] Q.J. Pan, On the manufacturing methods and developing prospect of manganic manganous oxide (Mn_3O_4), *China's Manganese Industry* 16 (1998) 51–55.
- [18] N. Serpone, D. Lawless, R. Khairutdinov, Size effects on the photophysical properties of colloidal anatase TiO_2 particles: size quantization or direct transitions in this indirect semiconductor?, *Journal of Physical Chemistry* 99 (1995) 16646–16654.
- [19] P. Parhi, T.N. Karthik, V. Manivannan, Synthesis and characterization of metal tungstates by novel solid-state metathetic approach, *Journal of Alloys and Compounds* 465 (2008) 380–386.